

## Form Factor Ratio Measurement in $\Lambda_c^+ \rightarrow \Lambda e^+ \nu_e$

G. Crawford,<sup>1</sup> C. M. Daubemier,<sup>1</sup> R. Fulton,<sup>1</sup> D. Fujino,<sup>1</sup> K. K. Gan,<sup>1</sup> K. Honscheid,<sup>1</sup> H. Kagan,<sup>1</sup> R. Kass,<sup>1</sup> J. Lee,<sup>1</sup> M. Sung,<sup>1</sup> C. White,<sup>1</sup> A. Wolf,<sup>1</sup> M. M. Zoeller,<sup>1</sup> F. Butler,<sup>2</sup> X. Fu,<sup>2</sup> B. Nemati,<sup>2</sup> W. R. Ross,<sup>2</sup> P. Skubic,<sup>2</sup> M. Wood,<sup>2</sup> M. Bishai,<sup>3</sup> J. Fast,<sup>3</sup> E. Gerndt,<sup>3</sup> J. W. Hinson,<sup>3</sup> R. L. McIlwain,<sup>3</sup> T. Miao,<sup>3</sup> D. H. Miller,<sup>3</sup> M. Modesitt,<sup>3</sup> D. Payne,<sup>3</sup> E. I. Shibata,<sup>3</sup> I. P. J. Shipsey,<sup>3</sup> P. N. Wang,<sup>3</sup> M. Battle,<sup>4</sup> J. Ernst,<sup>4</sup> L. Gibbons,<sup>4</sup> Y. Kwon,<sup>4</sup> S. Roberts,<sup>4</sup> E. H. Thorndike,<sup>4</sup> C. H. Wang,<sup>4</sup> J. Dominick,<sup>5</sup> M. Lambrecht,<sup>5</sup> S. Sanghera,<sup>5</sup> V. Shelkov,<sup>5</sup> T. Skwarnicki,<sup>5</sup> R. Stroynowski,<sup>5</sup> I. Volobouev,<sup>5</sup> G. Wei,<sup>5</sup> P. Zadorozhny,<sup>5</sup> M. Artuso,<sup>6</sup> M. Gao,<sup>6</sup> M. Goldberg,<sup>6</sup> D. He,<sup>6</sup> N. Horwitz,<sup>6</sup> G. C. Moneti,<sup>6</sup> R. Mountain,<sup>6</sup> F. Muheim,<sup>6</sup> Y. Mukhin,<sup>6</sup> S. Playfer,<sup>6</sup> Y. Rozen,<sup>6</sup> S. Stone,<sup>6</sup> X. Xing,<sup>6</sup> G. Zhu,<sup>6</sup> J. Bartelt,<sup>7</sup> S. E. Csorna,<sup>7</sup> Z. Egyed,<sup>7</sup> V. Jain,<sup>7</sup> D. Gibaut,<sup>8</sup> K. Kinoshita,<sup>8</sup> P. Pomianowski,<sup>8</sup> B. Barish,<sup>9</sup> M. Chadha,<sup>9</sup> S. Chan,<sup>9</sup> D. F. Cowen,<sup>9</sup> G. Eigen,<sup>9</sup> J. S. Miller,<sup>9</sup> C. O'Grady,<sup>9</sup> J. Urheim,<sup>9</sup> A. J. Weinstein,<sup>9</sup> M. Athanas,<sup>10</sup> W. Brower,<sup>10</sup> G. Masek,<sup>10</sup> H. P. Paar,<sup>10</sup> J. Gronberg,<sup>11</sup> C. M. Korte,<sup>11</sup> R. Kutschke,<sup>11</sup> S. Menary,<sup>11</sup> R. J. Morrison,<sup>11</sup> S. Nakanishi,<sup>11</sup> H. N. Nelson,<sup>11</sup> T. K. Nelson,<sup>11</sup> C. Qiao,<sup>11</sup> J. D. Richman,<sup>11</sup> A. Ryd,<sup>11</sup> D. Sperka,<sup>11</sup> H. Tajima,<sup>11</sup> M. S. Witherell,<sup>11</sup> M. Procaro,<sup>12</sup> R. Balest,<sup>13</sup> K. Cho,<sup>13</sup> W. T. Ford,<sup>13</sup> D. R. Johnson,<sup>13</sup> K. Lingel,<sup>13</sup> M. Lohner,<sup>13</sup> P. Rankin,<sup>13</sup> J. G. Smith,<sup>13</sup> J. P. Alexander,<sup>14</sup> C. Bebek,<sup>14</sup> K. Berkelman,<sup>14</sup> K. Bloom,<sup>14</sup> T. E. Browder,<sup>14,\*</sup> D. G. Cassel,<sup>14</sup> H. A. Cho,<sup>14</sup> D. M. Coffman,<sup>14</sup> D. S. Croccroft,<sup>14</sup> P. S. Drell,<sup>14</sup> D. J. Dumas,<sup>14</sup> R. Ehrlich,<sup>14</sup> P. Gaidarev,<sup>14</sup> M. Garcia-Sciveres,<sup>14</sup> B. Geiser,<sup>14</sup> B. Gittelman,<sup>14</sup> S. W. Gray,<sup>14</sup> D. L. Hartill,<sup>14</sup> B. K. Heltsley,<sup>14</sup> S. Henderson,<sup>14</sup> C. D. Jones,<sup>14</sup> S. L. Jones,<sup>14</sup> J. Kandaswamy,<sup>14</sup> N. Katayama,<sup>14</sup> P. C. Kim,<sup>14</sup> D. L. Kreinick,<sup>14</sup> G. S. Ludwig,<sup>14</sup> J. Masui,<sup>14</sup> J. Mevissen,<sup>14</sup> N. B. Mistry,<sup>14</sup> C. R. Ng,<sup>14</sup> E. Nordberg,<sup>14</sup> J. R. Patterson,<sup>14</sup> D. Peterson,<sup>14</sup> D. Riley,<sup>14</sup> S. Salman,<sup>14</sup> M. Sapper,<sup>14</sup> F. Würthwein,<sup>14</sup> P. Avery,<sup>15</sup> A. Freyberger,<sup>15</sup> J. Rodriguez,<sup>15</sup> S. Yang,<sup>15</sup> J. Yelton,<sup>15</sup> D. Cinabro,<sup>16</sup> T. Liu,<sup>16</sup> M. Saulnier,<sup>16</sup> R. Wilson,<sup>16</sup> H. Yamamoto,<sup>16</sup> T. Bergfeld,<sup>17</sup> B. I. Eisenstein,<sup>17</sup> G. Gollin,<sup>17</sup> B. Ong,<sup>17</sup> M. Palmer,<sup>17</sup> M. Selen,<sup>17</sup> J. J. Thaler,<sup>17</sup> K. W. Edwards,<sup>18</sup> M. Ogg,<sup>18</sup> A. Bellerive,<sup>19</sup> D. I. Britton,<sup>19</sup> E. R. F. Hyatt,<sup>19</sup> D. B. MacFarlane,<sup>19</sup> P. M. Patel,<sup>19</sup> B. Spaan,<sup>19</sup> A. J. Sadoff,<sup>20</sup> R. Ammar,<sup>21</sup> P. Baringer,<sup>21</sup> A. Bean,<sup>21</sup> D. Besson,<sup>21</sup> D. Coppage,<sup>21</sup> N. Coptly,<sup>21</sup> R. Davis,<sup>21</sup> N. Hancock,<sup>21</sup> M. Kelly,<sup>21</sup> S. Kotov,<sup>21</sup> I. Kravchenko,<sup>21</sup> N. Kwak,<sup>21</sup> H. Lam,<sup>21</sup> Y. Kubota,<sup>22</sup> M. Lattery,<sup>22</sup> M. Momayezi,<sup>22</sup> J. K. Nelson,<sup>22</sup> S. Patton,<sup>22</sup> R. Poling,<sup>22</sup> V. Savinov,<sup>22</sup> S. Schrenk,<sup>22</sup> R. Wang,<sup>22</sup> M. S. Alam,<sup>23</sup> I. J. Kim,<sup>23</sup> Z. Ling,<sup>23</sup> A. H. Mahmood,<sup>23</sup> J. J. O'Neill,<sup>23</sup> H. Severini,<sup>23</sup> C. R. Sun,<sup>23</sup> and F. Wappler<sup>23</sup>

(CLEO Collaboration)

<sup>1</sup>Ohio State University, Columbus, Ohio 43210

<sup>2</sup>University of Oklahoma, Norman, Oklahoma 73019

<sup>3</sup>Purdue University, West Lafayette, Indiana 47907

<sup>4</sup>University of Rochester, Rochester, New York 14627

<sup>5</sup>Southern Methodist University, Dallas, Texas 75275

<sup>6</sup>Syracuse University, Syracuse, New York 13244

<sup>7</sup>Vanderbilt University, Nashville, Tennessee 37235

<sup>8</sup>Virginia Polytechnic Institute and State University, Blacksburg, Virginia 24061

<sup>9</sup>California Institute of Technology, Pasadena, California 91125

<sup>10</sup>University of California, San Diego, La Jolla, California 92093

<sup>11</sup>University of California, Santa Barbara, California 93106

<sup>12</sup>Carnegie Mellon University, Pittsburgh, Pennsylvania 15213

<sup>13</sup>University of Colorado, Boulder, Colorado 80309-0390

<sup>14</sup>Cornell University, Ithaca, New York 14853

<sup>15</sup>University of Florida, Gainesville, Florida 32611

<sup>16</sup>Harvard University, Cambridge, Massachusetts 02138

<sup>17</sup>University of Illinois, Champaign-Urbana, Illinois 61801

<sup>18</sup>Carleton University, Ontario, Canada K1S 5B6

and the Institute of Particle Physics, Montréal, Canada

<sup>19</sup>McGill University, Montréal, Québec, Canada H3A 2T8

and the Institute of Particle Physics, Montréal, Canada

<sup>20</sup>Ithaca College, Ithaca, New York 14850

<sup>21</sup>University of Kansas, Lawrence, Kansas 66045

<sup>22</sup>University of Minnesota, Minneapolis, Minnesota 55455

<sup>23</sup>State University of New York at Albany, Albany, New York 12222

(Received 13 January 1995)

The angular distributions of the decay  $\Lambda_c^+ \rightarrow \Lambda e^+ \nu_e$  have been studied using the CLEO II detector. By performing a three-dimensional maximum likelihood fit, the form factor ratio  $R = f_2/f_1$  is determined to be  $-0.25 \pm 0.14 \pm 0.08$ . The decay asymmetry parameter of the  $\Lambda_c$  averaged over  $q^2$  is calculated to be  $\alpha_{\Lambda_c} = -0.82^{+0.09+0.06}_{-0.06-0.03}$ .

PACS numbers: 13.30.Ce, 14.20.Lq

Charm semileptonic decays allow a measurement of the form factors which parametrize the hadronic current because the Cabibbo-Kobayashi-Maskawa (CKM) matrix element  $|V_{cs}|$  is known from unitarity [1]. Within heavy quark effective theory (HQET) [2],  $\Lambda$ -type baryons are more straightforward to treat than mesons as they consist of a heavy quark and a spin and isospin zero light diquark. This simplicity allows for more reliable predictions concerning heavy quark to light quark transitions [3,4] than is the case for mesons. A measurement of the form factors in  $\Lambda_c^+ \rightarrow \Lambda e^+ \nu_e$  will help the future determination of the matrix element  $V_{ub}$  using  $\Lambda_b$  decays since HQET relates the form factors in  $\Lambda_c$  decay to those governing  $\Lambda_b$  semileptonic decays.

In the limit of negligible lepton mass, the semileptonic decay of a charmed baryon ( $1/2^+ \rightarrow 1/2^+$ ) is usually parametrized in terms of four form factors: two axial form factors  $F_1^A$  and  $F_2^A$  and two vector form factors  $F_1^V$  and

$F_2^V$ . These form factors are functions of  $q^2$ , the invariant mass squared of the virtual  $W$ . In the zero lepton mass approximation, the decay may be described in terms of helicity amplitudes  $H_{\lambda_\Lambda \lambda_W} = H_{\lambda_\Lambda \lambda_W}^V + H_{\lambda_\Lambda \lambda_W}^A$ , where  $\lambda_\Lambda$  and  $\lambda_W$  are the helicities of the  $\Lambda$  and  $W$ . The helicity amplitudes are related to the form factors by [4]

$$\begin{aligned} \sqrt{q^2} H_{(1/2)0}^V &= \sqrt{Q_-} [(M_{\Lambda_c} + M_\Lambda) F_1^V - q^2 F_2^V], \\ H_{(1/2)1}^V &= \sqrt{2Q_-} [-F_1^V + (M_{\Lambda_c} + M_\Lambda) F_2^V], \\ \sqrt{q^2} H_{(1/2)0}^A &= \sqrt{Q_+} [(M_{\Lambda_c} - M_\Lambda) F_1^A + q^2 F_2^A], \\ H_{(1/2)1}^A &= \sqrt{2Q_+} [-F_1^A - (M_{\Lambda_c} - M_\Lambda) F_2^A], \end{aligned} \quad (1)$$

where  $Q_\pm = (M_{\Lambda_c} \pm M_\Lambda)^2 - q^2$ . The remaining helicity amplitudes can be obtained using the parity relations  $H_{-\lambda_\Lambda - \lambda_W}^{V(A)} = +(-)H_{\lambda_\Lambda \lambda_W}^{V(A)}$ . In terms of the helicity amplitudes, the decay angular distribution can be written as [4]

$$\begin{aligned} \Gamma_S &= \frac{d\Gamma}{dq^2 d \cos\Theta_W d \cos\Theta_\Lambda} = B(\Lambda \rightarrow p\pi) \frac{1}{2} \frac{G_F^2}{(2\pi)^4} |V_{cs}|^2 \frac{q^2 P}{24M_{\Lambda_c}^2} \\ &\times \left\{ \frac{3}{8} (1 - \cos\Theta_W)^2 |H_{(1/2)1}|^2 (1 + \alpha_\Lambda \cos\Theta_\Lambda) + \frac{3}{8} (1 + \cos\Theta_W)^2 |H_{(-1/2)-1}|^2 (1 - \alpha_\Lambda \cos\Theta_\Lambda) \right. \\ &\left. + \frac{3}{4} \sin^2 \Theta_W [|H_{(1/2)0}|^2 (1 + \alpha_\Lambda \cos\Theta_\Lambda) + |H_{(-1/2)0}|^2 (1 - \alpha_\Lambda \cos\Theta_\Lambda)] \right\}, \end{aligned} \quad (2)$$

where  $G_F$  is the Fermi coupling constant,  $V_{cs}$  is the CKM matrix element,  $P$  is the  $\Lambda$  momentum in the  $\Lambda_c$  rest frame,  $\Theta_\Lambda$  is the angle between the momentum vector of the proton in the  $\Lambda$  rest frame and the  $\Lambda$  momentum in the  $\Lambda_c$  rest frame,  $\Theta_W$  is the angle between the momentum vector of the positron in the  $W$  rest frame and the  $\Lambda$  momentum in the  $\Lambda_c$  rest frame, and  $\alpha_\Lambda$  is the  $\Lambda \rightarrow p\pi$  decay asymmetry parameter measured to be  $0.64 \pm 0.01$  [1].

Within the framework of HQET the heavy flavor and spin symmetries imply relations among the form factors which reduce their number to one when the decay involves only heavy quarks. In this Letter we follow Ref. [4] where it is argued that the HQET formalism may also work for  $\Lambda_c^+ \rightarrow \Lambda e^+ \nu_e$ . Treating the  $c$  quark as a heavy quark, two independent form factors  $f_1$  and  $f_2$  are required to describe the hadronic current. The relationships between these form factors and the standard form factors are  $F_1^V(q^2) = -F_1^A(q^2) = f_1(q^2) + (M_\Lambda/M_{\Lambda_c})f_2(q^2)$  and  $F_2^V(q^2) = -F_2^A(q^2) = (1/M_{\Lambda_c})f_2(q^2)$ . In general  $f_2$  is

expected to be negative and smaller in magnitude than  $f_1$ . If the strange quark is treated as heavy,  $f_2$  is zero.

In order to extract the form factor ratio  $R = f_2/f_1$  from a fit to  $\Gamma_S$  an assumption must be made about the  $q^2$  dependence of the form factors. We follow the model of Körner and Krämer (KK) [4] who use the dipole form  $f(q^2) = f(q_{\max}^2)(1 - q_{\max}^2/m_{ff}^2)^2/(1 - q^2/m_{ff}^2)^2$ , where the pole mass is chosen to be  $m_{ff} = 2.11 \text{ GeV}/c^2$ . With the current statistical power, the angular distributions are not sensitive to the  $q^2$  dependence of the form factors.

The data sample used in this study was collected with the CLEO II detector [5] at the Cornell Electron Storage Ring (CESR). The integrated luminosity consists of  $3.0 \text{ fb}^{-1}$  taken at and just below the  $\Upsilon(4S)$  resonance, corresponding to approximately  $4 \times 10^6$   $e^+e^- \rightarrow c\bar{c}$  events. We search for the decay  $\Lambda_c^+ \rightarrow \Lambda e^+ \nu_e$  in  $e^+e^- \rightarrow c\bar{c}$  events by detecting a  $\Lambda e^+$  pair with invariant mass in the range  $m_\Lambda < m_{\Lambda e^+} < m_{\Lambda_c}$  [6]. All tracks are required to come from the region of the event vertex. To reduce the background from  $B$  decays, we require

$R_2 = H_2/H_0 > 0.2$ , where  $H_i$  are Fox-Wolfram event shape variables [7]. Positrons are identified using a likelihood function which incorporates information from the calorimeter and  $dE/dx$  systems. The minimum allowed momentum for positron candidates is  $0.7 \text{ GeV}/c$ . Positrons are required to have been detected in the region  $|\cos\theta| < 0.71$ , where  $\theta$  is the angle between the positron momentum and the beam line.

The  $\Lambda$  is reconstructed through its decay to  $p\pi$ . We require the point of intersection of the two charged tracks, measured in the  $r$ - $\phi$  plane, to be greater than  $0.5 \text{ cm}$  away from the primary vertex. In addition, we require the sum of the  $p$  and  $\pi$  momentum vectors to extrapolate back to the beam line. The  $dE/dx$  measurement of the proton is required to be consistent with the expected value. We reject combinations which satisfy interpretation as a  $K_s^0$ . Finally, we require the momentum of the  $p\pi$  pair to be greater than  $0.8 \text{ GeV}/c$  in order to reduce combinatoric background. These  $\Lambda$  candidates are then combined with positrons, and the sum of the  $\Lambda$  and  $e^+$  momenta,  $p_{\Lambda e^+}$ , is required to be greater than  $1.4 \text{ GeV}/c$ . This cut reduces our dependence on the shape of the  $\Lambda_c$  fragmentation function at low momentum, which is poorly known.

The number of events passing these requirements is 1076, of which  $137 \pm 12$  are consistent with fake  $\Lambda$  background,  $120 \pm 36$  are consistent with fake positron background, and  $106 \pm 21$  with  $\Xi_c \rightarrow \Xi e^+ \nu_e$  and  $\Xi \rightarrow \Lambda(\pi)$  feedthrough. Details of the background estimates can be found in a previous paper [8]. The sidebands of the  $p\pi$  invariant mass distribution are used to estimate the fake  $\Lambda$  background in this study [9]. The fake positron background is estimated using events containing a  $\Lambda$  candidate by multiplying the number of tracks satisfying our kinematic criteria which are not positively identified as a positron with the probability for a hadron to be identified as a positron. The background from  $\Xi_c \rightarrow \Xi e^+ \nu_e$  decays is estimated using the result of a previous analysis [10]. With the selection criteria described above, we find no evidence for  $\Lambda e^+ \nu_e$  final states in which there are additional  $\Lambda_c^+$  decay products [8]. In Fig. 1, we show the  $m_{\Lambda e^+}$  distribution after  $\Lambda$  sideband subtraction and comparisons between the data and Monte Carlo (MC) distributions.

Calculating kinematic variables requires knowledge of the  $\Lambda_c$  momentum which is unknown due to the undetected neutrino. The direction of the  $\Lambda_c$  is approximated by the thrust axis of the event. The magnitude of the  $\Lambda_c$  momentum is then obtained by solving the equation  $\vec{P}_{\Lambda_c}^2 = (\vec{P}_\Lambda + \vec{P}_e + \vec{P}_{\nu_e})^2$ . We determine the best solution by MC simulation following the procedure described in detail in Ref. [8]. After the  $\Lambda_c$  momentum is estimated, the three kinematic variables are obtained by working in the  $\Lambda_c$  center-of-mass frame. The resolutions on  $q^2/q_{\text{max}}^2$ ,  $\cos\Theta_\Lambda$ , and  $\cos\Theta_W$  determined by MC are 0.25, 0.25, and 0.2, respectively.

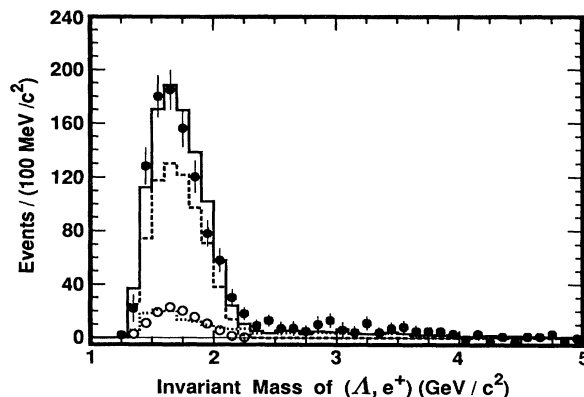


FIG. 1. Invariant  $\Lambda e^+$  mass for right sign combinations. The points with error bars are data after subtraction of the contribution of fake  $\Lambda$ 's estimated using the  $p\pi$  invariant mass sidebands. The dotted line and the open circles show the fake positron and the feedthrough backgrounds, respectively. The dashed line shows the MC prediction for  $\Lambda_c^+ \rightarrow \Lambda e^+ \nu_e$  normalized to the data after subtraction of the backgrounds. The solid line shows the sum of the MC prediction and the backgrounds.

Using  $q^2/q_{\text{max}}^2$ ,  $\cos\Theta_\Lambda$ , and  $\cos\Theta_W$ , we perform a three-dimensional unbinned maximum likelihood fit in a manner similar to Ref. [11]. This technique enables a multidimensional likelihood fit to be performed to variables modified by experimental acceptance and resolution and is necessary for this analysis due to the substantial smearing of the kinematic variables. The essence of the method is to determine the probability density function by using the population of appropriately weighted MC events in the three-dimensional kinematic space. This is accomplished by generating one high statistics sample of MC events with a known value of the form factor ratio  $R$  and corresponding known values of the three kinematic variables  $q^2/q_{\text{max}}^2$ ,  $\cos\Theta_\Lambda$ , and  $\cos\Theta_W$  for each event. The generated events are then processed through the full detector simulation, off-line analysis programs, and selection criteria. Using the generated kinematic variables, the accepted MC events are weighted by the ratio of the decay distribution for the trial values of  $R$  to that of the generated distribution. The accepted MC events are now, therefore, distributed according to the probability density corresponding to the trial values of  $R$ . By such weighting, a likelihood may be evaluated for each data event for different values of the form factor ratio, and a fit performed. The probability for each event is determined by sampling this distribution using a search volume around each data point. The volume size is chosen so that the systematic effect from finite search volumes is small and the required number of MC events is not prohibitively high.

The  $\Lambda_c^+ \rightarrow \Lambda e^+ \nu_e$  sample has signal to background in the approximate ratio 2:1. Background is incorporated into the fitting technique by constructing the

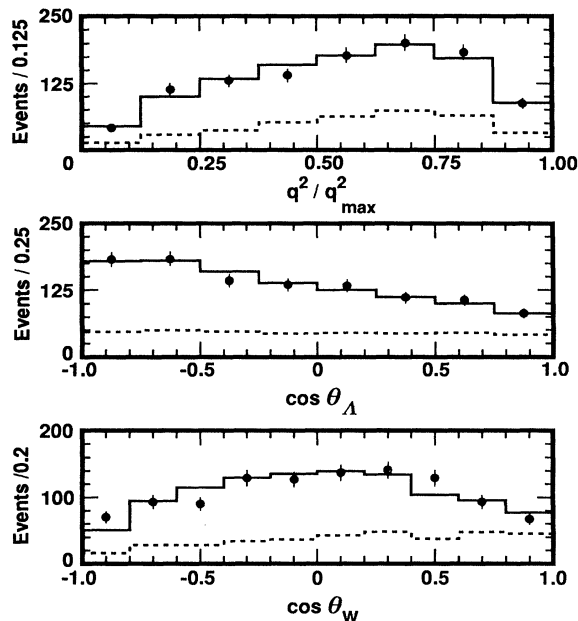


FIG. 2. Projections to the data (points with error bars) and the fit (solid histogram) for  $q^2/q_{\max}^2$ ,  $\cos\Theta_{\Lambda}$ , and  $\cos\Theta_W$ . The dashed lines show the background distributions.

log-likelihood function  $\ln \mathcal{L} = \sum_{i=1}^N \ln(P_S \Gamma_S + P_B \Gamma_B)$ , where  $N$  is the number of events in the signal region,  $P_S$  and  $P_B$  are the probabilities that events in this region are signal and background, respectively,  $\Gamma_S$  is the signal shape modeled from signal MC, and  $\Gamma_B$  is the background shape modeled by the background samples. Fake positron background is modeled by the fake positron data sample. Feedthrough background from  $\Xi_c \rightarrow \Xi e^+ \nu_e$  is modeled by the MC sample which is generated according to the HQET-consistent KK model. Fake  $\Lambda$  background is modeled using data events in the sidebands of the  $p\pi$  invariant mass distribution.

Using the above method we find  $R = -0.25 \pm 0.14$  where the error is statistical. The confidence level of the fit is determined to be 15% using the method of nearest neighbors [12]. Figures 2 and 3 show the projections of the  $q^2/q_{\max}^2$ ,  $\cos\Theta_{\Lambda}$ , and  $\cos\Theta_W$  distributions for the data and for the fit.

We have considered the following sources of systematic error and give our estimate of their magnitude in parentheses. The statistical error in the MC sample is estimated by dividing the MC into three equal parts and repeating the fit (0.02). The error due to the search volume size is determined by varying the size of the search volume (0.04). The errors due to background normalization and shape are determined by varying the estimated number of the background events in the signal region by one standard deviation and by using different background samples (0.03). The error associated with the

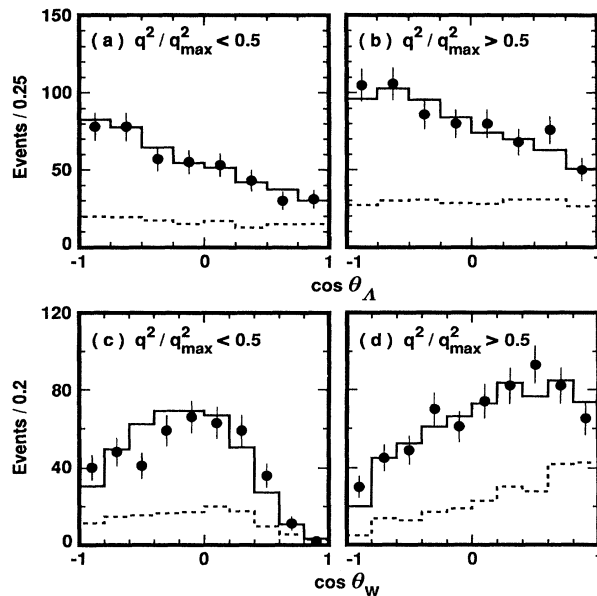


FIG. 3. Projections of the data (points with error bars) and the fit (solid histogram) onto  $\cos\Theta_{\Lambda}$  and  $\cos\Theta_W$  for different  $q^2/q_{\max}^2$  regions. The dashed lines show the background distributions.

ratio of form factors for the decay of  $\Xi_c \rightarrow \Xi e^+ \nu_e$  is determined by varying this ratio and repeating the fit (0.04). As this measurement is insensitive to the production polarization  $\mathcal{P}$  of the  $\Lambda_c$  no systematic error has been included from this source [13]. The sensitivity to the  $q^2$  dependence is also investigated by using functional forms other than the dipole form and by using a modified dipole form which gives mildly different  $q^2$  dependences for  $f_1$  and  $f_2$ . The variation of the value of  $R$  derived from these different fits is found to be small and no systematic error has been included. The error associated with the uncertainty in the  $\Lambda_c$  fragmentation function is estimated by varying this function (0.01). The error associated with MC modeling of slow pions from  $\Lambda$  decay is obtained by varying this efficiency according to our understanding of the CLEO II detector (0.01). To estimate the error associated with the technique of incorporating background into the fit, two other methods of computing the log-likelihood ratio are used: direct background subtraction and a hybrid of the method outlined earlier and direct subtraction. The difference between the central values found by these three methods (0.03) is taken as the systematic error. Adding all sources of systematic error in quadrature we find  $R = -0.25 \pm 0.14 \pm 0.08$ .

Using the value of  $R$  obtained here and the HQET-consistent KK model, the mean value of the decay asymmetry parameter of  $\Lambda_c^+ \rightarrow \Lambda e^+ \nu_e$  is calculated to be  $\alpha_{\Lambda_c} = -0.82^{+0.09+0.06}_{-0.06-0.03}$ . The average value of  $q^2$  in the KK model ( $R = -0.25$ ) is  $0.7 (\text{GeV}/c^2)^2$ . This

is consistent with our previous measurement of  $\alpha_{\Lambda_c}$  determined from the  $\cos\Theta_\Lambda$  distribution [8] but has a smaller error since it is obtained using more experimental information and additional data.

In conclusion, using a three-dimensional maximum likelihood fit the angular distributions of  $\Lambda_c^+ \rightarrow \Lambda e^+ \nu_e$  have been studied and the form factor ratio  $R = f_2/f_1$  is found to be  $-0.25 \pm 0.14 \pm 0.08$ . At the current level of experimental sensitivity the hadronic matrix element in the semileptonic decay of the  $\Lambda_c$  baryon is adequately described by two form factors as predicted by HQET.

We gratefully acknowledge the effort of the CESR staff in providing us with excellent luminosity and running conditions. This work was supported by the National Science Foundation, the U.S. Department of Energy, the Heisenberg Foundation, the SSC Fellowship program of TNRLX, Natural Sciences and Engineering Research Council of Canada, and the A. P. Sloan Foundation.

---

\*Permanent address: University of Hawaii at Manoa, Honolulu, HI 96822-2219.

- [1] Particle Data Group, Phys. Rev. D **50**, 1 (1994).  $|V_{cs}|$  is determined only from unitarity in a standard model with three generations.
- [2] N. Isgur and M. B. Wise, Phys. Lett. B **232**, 113 (1989); **237**, 527 (1990); E. Eichten and B. Hill, Phys. Lett. B **234**, 511 (1990); H. Georgi, Phys. Lett. B **240**, 447 (1990).
- [3] T. Mannel, W. Roberts, and Z. Ryzak, Nucl. Phys. **B355**, 38 (1991); Phys. Lett. B **255**, 593 (1991); F. Hussain, J. G. Körner, M. Krämer, and G. Thompson, Z. Phys. C **51**, 321 (1991); A. F. Falk and M. Neubert, Phys. Rev. D **47**, 2982 (1993); H. Georgi, B. Grinstein, and M. B. Wise, Phys. Lett. B **252**, 456 (1990); N. Isgur and M. B. Wise, Nucl. Phys. **B348**, 276 (1991); H. Georgi, Nucl. Phys. **B348**, 293 (1991).
- [4] J. G. Körner and M. Krämer, Phys. Lett. B **275**, 495 (1992).
- [5] Y. Kubota *et al.*, Nucl. Instrum. Methods Phys. Res., Sect. A **320**, 255 (1992).
- [6] Throughout this paper charge conjugate modes are implicitly included.
- [7] G. C. Fox and S. Wolfram, Phys. Rev. Lett. **41**, 1581 (1978).
- [8] CLEO Collaboration, T. Bergfeld *et al.*, Phys. Lett. B **323**, 219 (1994).
- [9] In Ref. [8] the fake  $\Lambda$  background was allowed for by fitting the  $p\pi$  invariant mass. The  $\Lambda$  sideband method used in this work gives a consistent estimate of the fake  $\Lambda$  background.
- [10] CLEO Collaboration, J. Alexander *et al.*, CLNS 94 /1288 (to be published).
- [11] D. M. Schmidt, R. J. Morrison, and M. S. Witherell, Nucl. Instrum. Methods Phys. Res., Sect. A **328**, 547 (1993).
- [12] J. H. Friedman, CERN Report No. 74-23 271, 1974.
- [13] Parity conservation in the electromagnetic and strong interaction requires  $\Lambda_c$  production polarization to be normal to the production plane, and charge conjugation invariance requires the sign of the polarization to be the same for particle and antiparticle. Since  $\alpha_{\Lambda_c}$  is  $CP$  odd,  $(\alpha_{\Lambda_c} \mathcal{P})$  is  $CP$  odd so that averaged over charge conjugate states the net polarization is zero.